Pneumatic Conveying

Edward J. Bissaker[1] Ognjen Orozovic[2]
Michael H. Meylan[3] Fillipe Georgiou[4] Tomas J. Marsh[5]
James M. Hill[6] Mark J. McGuinness[7]
Winston L. Sweatman[8] Ngamta Thamwattana[9]

(Received 29 June 2021; revised 27 April 2023)

Abstract

Pneumatic conveying is the transportation of bulk solids in enclosed pipelines via a carrier gas, typically air. The local flow pattern in a pipeline is a function of the conditions, and slug flow can form under certain conditions. Slug flow is a naturally occurring, wave-like flow where the bulk material travels along the pipeline in distinct 'slugs'. Establishing the environment for the formation of slugs within the conveying system is essential to maximise the overall system efficiency and minimise damage to the bulk material. MISG2021 considered a wide range of mathematical approaches to slug formation and travel. These two key problem areas have the most significant potential to impact the system design and efficiency. Critical interconnected facets of pneumatic conveying systems were investigated and an overview for

DOI:10.21914/anziamj.v63.16615, © Austral. Mathematical Soc. 2023. Published 2023-05-11, as part of the Proceedings of the 2021 Mathematics and Statistics in Industry Study Group. ISSN 1445-8810. (Print two pages per sheet of paper.) Copies of this article must not be made otherwise available on the internet; instead link directly to the DOI for this article.

future work was developed. Many of the avenues uncovered during the MISG2021 require more time for in-depth analysis. This analysis and framework will aid in optimising conveying system design and provide insight to construct more efficient pneumatic conveying systems.

Contents

1 Introduction **M7**

2 Slug Formation **M10**
2.1 Mass Transport M11
2.2 Sand Dunes M16

3 Slug Travel and Motion **M19**
3.1 Velocity of the Slug M19
3.2 A Closed-form Solution M19
3.3 Permeating flow rate M25

4 Conclusions and Future Work **M28**
4.1 Future Work M28
4.2 Conclusions M30

1 Introduction

The problem brought to MISG2021, held at the University of Newcastle in person and online, was to model slug flow pneumatic conveying, specifically, the formation of slugs and their motion. Pneumatic conveying is the transportation of bulk solids in pipelines via a carrier gas, typically air. While not as energy efficient as mechanical conveyors, such as belts, pneumatic conveyors offer several unique advantages. The low number of moving parts makes pneumatic conveyors relatively simple and economical to maintain.

The option for flexible routing through bends is another significant advantage over mechanical conveyors. The enclosed nature of the conveying is why over 50% of industrial applications of pneumatic conveyors are found in the food and pharmaceutical industries (PCSMS 2019), where the need for isolating the conveyed material from the surrounding environment is greatest. However, pneumatic conveyors are also readily found in the mining, rubber, plastics and ceramics industries—with a combined global market size of US$25 billion in 2018 (PCSMS 2019). The local flow pattern in a pipeline depends on several interlinked variables, including the operating conditions regarding the amount of solids and gas fed into a pipeline, the bulk material properties, and the pipeline layout and geometry. However, globally the possible flow patterns are primarily dependent on the bulk material properties.

For materials with particles that are cohesionless (Tsuji, Tanaka, and Ishida 1992), have a narrow particle size distribution (Deng and Bradley 2016), and are of high sphericity (Hilton and Cleary 2011), the possible flow patterns are shown in Figure 1. This figure shows that a relative increase in the solids mass flow rate, or a decrease in the gas mass flow rate, results in more concentrated flows, culminating in slug flow.

Slug flow is a naturally occurring wave-like flow where the bulk material travels along the pipeline in distinct ‘slugs’. In horizontal pipelines the waves propagate through a stationary bed of material between slugs that partially fill the pipeline. While almost anything can be conveyed in a dilute phase, the disadvantages of this mode of transport are the high gas use and particle attrition or wear rates due to the high velocities. The higher solids concentrations and lower velocities of slug flow naturally remedy the disadvantages of dilute phase flow, albeit at the cost of a much more complicated and dynamic flow.

For slug flow, the many and often interlinked variables relating to operating conditions, bulk material properties, and pipeline parameters remain largely unknown. Because of this complexity, slug flow is often overlooked and replaced by less favourable dilute phase systems due to the increased reliability

Figure 1: Possible modes of flow for a bulk material capable of slug flow.

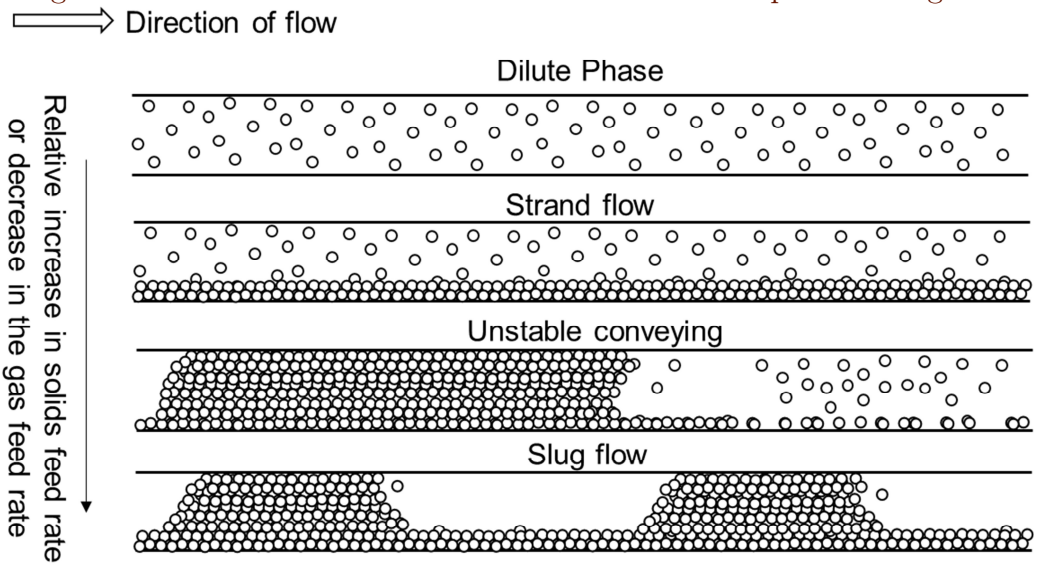

of dilute systems. Higher running costs for slug flow systems are intrinsically linked to a lack of understanding of slug flow's physical mechanisms. Hence, developing an effective slug flow system often relies on expensive one-to-one scale trials. Reliance on conveying trials and the development of methods centred around these trials means the field is highly empirical, and much of the theory surrounding dense system design, in general, is from models fitted to collected data (Shijo and Behera 2021). In many cases, design is experience-based, whereby an existing, reliable slug flow system is duplicated without considering differences in material properties or operating conditions. This is a problematic approach since published results demonstrate the importance of considering material properties in design (Deng and Bradley 2016; Hilton and Cleary 2011; Pan 1999; Pahk and Klinzing 2012; Li et al. 2014; Nied, Lindner, and Sommer 2017).

The complexity of the flow, coupled with development procedures that are heavily reliant on conveying trials and empiricism, generally means that

the modelling of slug flow has often resulted in oversimplification. Such a simplification is that the pressure drop in the air pockets between slugs is neglected since most pressure loss is over the slugs. Slugs can then be combined into a 'total' slug length, greatly simplifying the analysis. This simplification, along with analogies to fields such as porous media and bulk solids mechanics, has generally been the approach in most models (Konrad 1980; Mi and Wypych 1994; Pan and Wypych 1997; Yi 2001; Lecreps et al. 2014a; Shaul and Kalman 2015).

However, there are several obvious and nuanced issues with this approach. Firstly, combining slugs into a single length assumes linearity in the pressure drop with slug length. Validating this assumption is difficult with measurements due to the dynamic nature of slugs, and there is evidence to support linear (Pan and Wypych 1997) and nonlinear profiles (Lavrinec et al. 2019). Secondly, the analysis assumes existing slug structures are in a steady state. The steady assumption, along with combining slugs into a single length, immediately neglects the dynamic nature of individual slugs. Furthermore, assuming that the slug structures are already formed neglects how slugs begin in the first place. Consequently, slug formation mechanisms and slug dynamics have received little attention.

MISG2021 considered a wide range of mathematical approaches to the two key problem areas that have the most significant potential to quickly impact the system design and efficiency, which are conditions for slug formation and requirements for stable slug travel.

2 Slug Formation

Due to the reliance of most analysis tools on assuming steady conditions, transient phenomena have been largely understudied within the field. In systems that exhibit slug flow, the slug velocity consistently exceeds the velocity of the particles in the system (a travelling wave solution). This

behaviour is due to the particle exchanges between a slug and an underlying layer of solid material. Establishing the environment for the formation of slugs within the conveying system is vital to maximising the overall system efficiency. This section considers ideas and theories from related fields to better understand the situations that cause slugs to form. Futire investigation should provide some definitive relationships between the granular material and the optimal design of the conveying system. Such optimisations might include considering the influence of the pipeline radius, material (corresponding to wall friction and shear forces), and driving pressure. Due to the large number of parameters, the current empirical methods are not practical for testing all combinations. Therefore, any generalisations that may be obtained from a more fundamental modelling approach would be beneficial. This section focuses on slug formation, a natural starting point for assessing slug flow outside the typically assumed steady conditions.

2.1 Mass Transport

This section considers a momentum exchange principle to explain material deposition within the pneumatic conveying system, resulting in slug formation.

For the basis of this model, we consider an undisturbed fluid flowing within the conveying pipe. Due to the shear forces along the edges of the pipe, the velocity attains its maximum value at a location that maximises distance from the pipe walls (i.e., at the centre). Hence, before the addition of particles to the system, there exists velocity variation within the pipe. With the principle of momentum exchange, we assume that the velocity of a particle is proportional to the velocity of the gas in the nearby region. Therefore, pipe locations with the highest gas velocity correspond to particle transport, and low gas velocity areas become net deposition locations.

We see particles are most likely to collect along the bottom edge of the pipe, a region of low velocity where the potential for momentum exchange is lowest, and gravity provides a friction force. This assumption appears to be validated

by dilute phase flow only occurring within pneumatic conveying systems at high gas velocities (where momentum exchange close to walls is also high).

The disruption of the flow due to particulate matter causes the formation of a boundary layer. Understanding the shape of this boundary layer (i.e., the velocity/transport gradient) provides an understanding of how the tail end of the slug forms. Hence, the boundary layer can be used to determine optimal feed rates of material (to form this trailing tail edge) into the conveying system for a given gas velocity so that slugs form quickly and consistently.

We utilised a finite-element simulation of the Navier–Stokes equations to determine the effect of material deposition on the gas velocity. This simulation for a tube was constructed using the FEnics python module. In this simple simulation, we considered two different situations:

1. two small particles obstructing the gas stream;
2. a thin coating of material evenly distributed over the bottom of the pipe (represented by a rectangular region).

For simplicity, in both cases, the gas is treated as an incompressible fluid, which is reasonable given the sole purpose of demonstrating a velocity gradient.

Figures 2 and 3 show the introduction of material into the pipe causes the formation of a boundary layer, leading to a corresponding variation in the transport capacity of the fluid (corresponding to changes in velocity), responsible for the initial formation of the slug. We see from CFD-FEM simulation results for slug formation in Figure 3 by Hilton and Cleary (2011) that the areas of high velocity within the tube appear to correspond with the trailing edge of the slug. So the simple velocity mass transport model may provide some insight into the problem.

The finite element simulations provide insight into the variation in gas velocity due to material introduced into the tube. This velocity variation and the momentum exchange condition provide advection, and this links to the dirt pile conveyor problem by Stommel.

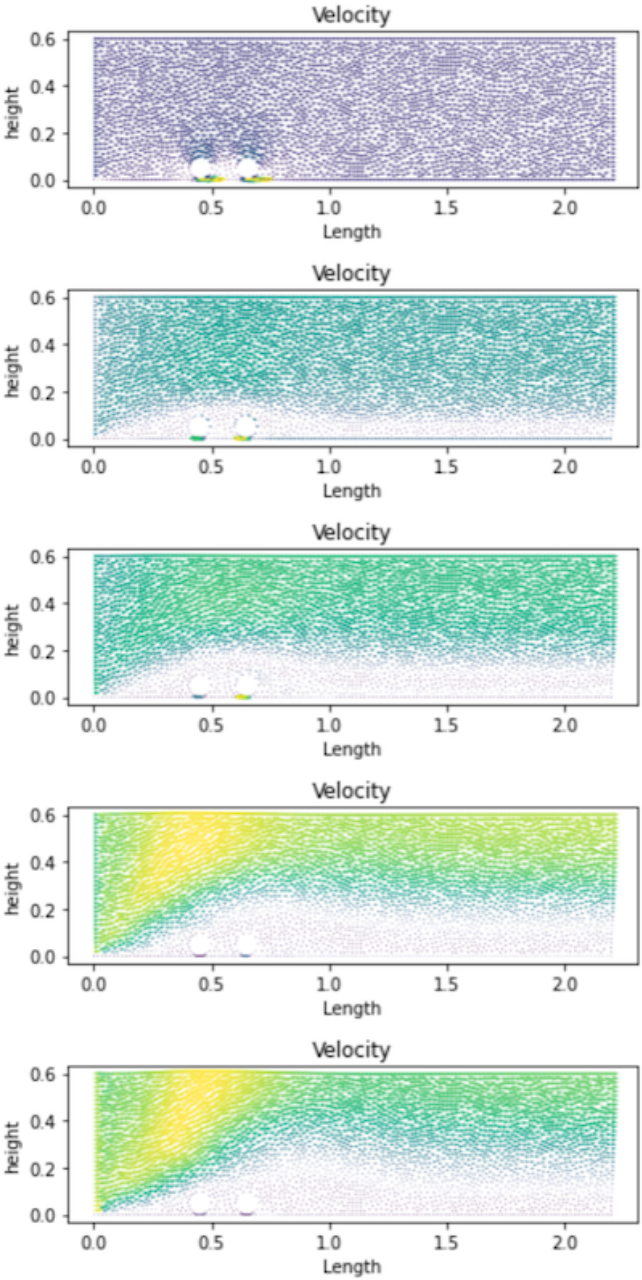

Figure 2: Changes to the velocity field along the tube caused by the two granular obstructions at the bottom of the pipe (and by granular approximation rectangle along the bottom of the tube in Figure 3). Top image is at $t = 0$, and the subsequent images are at one-second intervals.

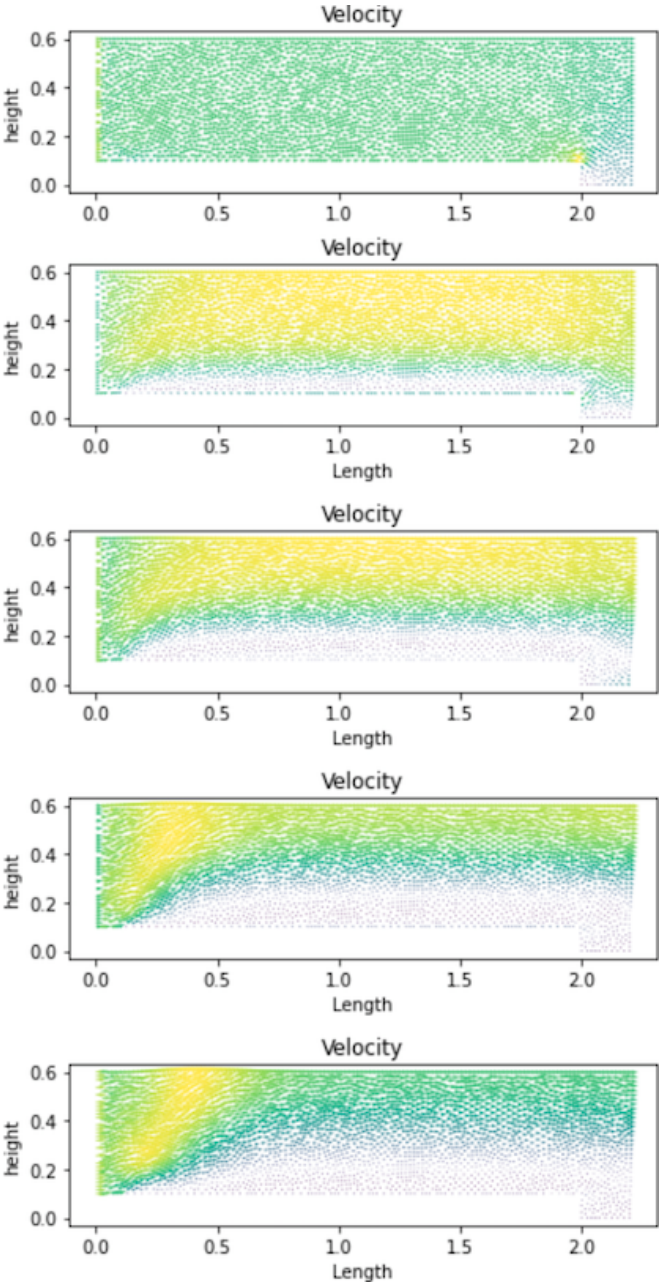

Figure 3: Changes to the velocity field along the tube caused by granular approximation rectangle along the bottom of the tube (and by two granular obstructions at the bottom of the pipe in Figure 2). Top image is at $t = 0$, and the subsequent images are at one-second intervals.

Stommel's dirtpile (Young 2016) considers the deposition of dirt into a pile with height $h(x,t)$, on a moving conveyor belt of length between $x=0$, $x=l$, modelled simply by

$$\frac{\partial h}{\partial t}+c\frac{\partial h}{\partial x}=s(x,t)+\kappa\frac{\partial^2 h}{\partial x^2}$$

for $s(x,t)$ the dirt deposition rate and c the conveyor speed. This equation is known to have travelling wave solutions, meeting the essential qualitative criteria of a slug in the pneumatic conveying system.

For a sufficiently large gas velocity (for high momentum exchange), the diffusion term for dirt in the pile, $\kappa\partial^2 h/\partial x^2$, should be excluded from the model. Incorporating the existence of the boundary layer demonstrated by the numerical simulation, we propose that this simple model could be used to determine slug formation and growth by changing c the conveying speed in Stommel's problem to be $c(t,h)$ a function of time and height within the tube. This function $c(t,h)$ represents the change of advection due to the variation in velocity within the pipe. It should be in qualitative agreement with the boundary layer demonstrated in the finite element simulation.

So the simple model becomes

$$\frac{\partial h}{\partial t}+c(t,h)\frac{\partial h}{\partial x}=s(x,t)$$

To determine if this simple model is appropriate would require us to define an expression for the boundary layer (velocity/transport capacity) as a function of the soil height h and time t. This step could be completed using an asymptotic method to determine an equation for velocity in the boundary layer. This velocity would then determine a transport capacity $c(t,h)$ given a known particle mass.

This momentum exchange model may provide valuable macrosystem insight into the optimal particle feed rate $s(x,t)$ to optimise the time taken for slug formation by maximising the pile size $h(x,t)$.

2.2 Sand Dunes

We now consider a naturally occurring mass transport system that demonstrates similar characteristics to the slugs and the gas-particle interface of sand dunes.

Bagnold (1941) conducted field observations and laboratory measurements in the 1930's to describe how wind over sand can produce ripples, ridges, and dunes. Dunes are larger in scale and asymmetrical, with the lee face (sheltered from the wind) being steeper and at the angle of repose (about 34°). Sand grains added to a face at the angle of repose form avalanches that cascade downwards so that the angle does not steepen. Further work, since Bagnold's seminal studies, indicates an instability occurs when the wind blows over a level sand surface, and that can produce sand dunes. Modelling predicts the most unstable wavelength. A subsequent model (Kennedy 1963), based on a result by Benjamin (1959) showed that, in a shear flow, the maximum shear stress at the bed is shifted upstream from the maximum elevation, thus providing an instability mechanism, transferring sand from the upwind slope to the top of a dune. An eddy viscosity model of the airflow has been used to study the instability (Engelund 1970; Smith 1970). The theory has been extended to the formation of ripples (Fredsøe 1974; Richards 1980), and continues to develop (Sumer and Bakioglu 1984; Colombini 2004; Charru and Hinch 2006).

The instability of air flowing over sand has been developed into a model for the nonlinear evolution of two and three-dimensional dunes by Herrmann and colleagues (Kroy, Sauermann, and Herrmann 2002; Parteli and Herrmann 2007; Parteli et al. 2009; Schwämmle and Herrmann 2004).

In all of these models, the conservation of sand for a bed at elevation $z = s(x, t)$ is expressed by the Exner equation

$$(1 - \phi)\frac{ds}{dt} + \frac{dq}{dx} = 0,$$

where ϕ is the porosity of the sand bed, and q is the sediment flux, which is

Figure 4: Toy sand dune profiles and the resulting stress. The lower set of three curves are arbitrary simple assumed dune profiles, and the upper set are resulting surface shear stresses $\tau(x)/\tau_0$. The wind is blowing from left to right. There is a small upwind shift of the maximum shear stress from the apex of the profiles at $x = 0$. (Reproduced with permission from Kroy, Sauermann, and Herrmann 2002, Figure 1).

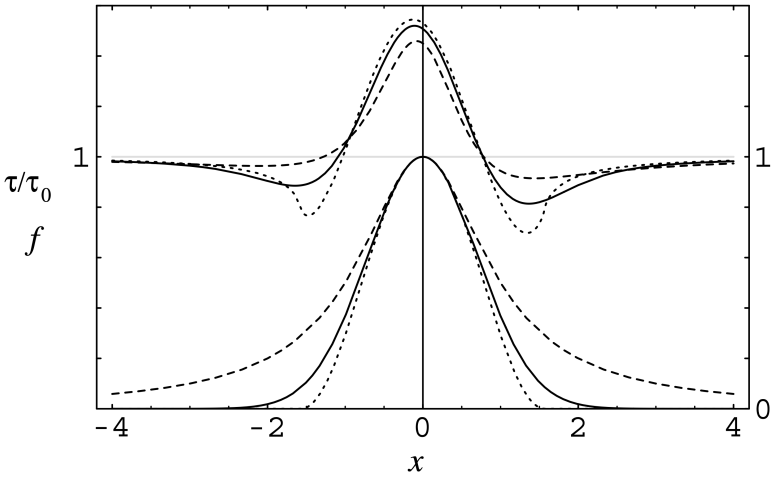

generally an increasing function of shear stress τ. A popular expression for q is $q = K(\tau - \tau_c)^{3/2}$, where τ_c is a critical value of shear stress for mobilisation (Meyer-Peter and Muller 1948). The shear stress τ is derived from the theory of Jackson and Hunt (1975). A logarithmic near-surface turbulent velocity profile gives the shear stress (Kroy, Sauermann, and Herrmann 2002) $\tau = \tau_0\left[1 - \alpha' H(s_x) + \beta' s_x\right]$, where H is the Hilbert transform, and τ_0 is the stress over the unperturbed bed.

This form for the stress crucially gives a maximum stress that is just upwind of the maximum of the dune shape, as illustrated for several particular choices of shape by Kroy, Sauermann, and Herrmann (2002) and reproduced here in Figure 4. The Hilbert transform, a convolution applied to the slope of the

sand surface, is the cause of this. Having the stress at a maximum just before the top of a dune causes the sand to move from the front of the dune to the back of the dune and not just erode the top.

Fowler (unpublished manuscript, 2011) modifies this by analysing the boundary-layer airflow Navier–Stokes equations, obtaining the Orr–Sommerfeld equation for the perturbed flow, which at large Reynolds number are solved to find an approximate shear stress

$$\tau = \frac{3\mu_T \overline{u}}{d}\left(1 - \frac{s}{d} + \frac{\mu}{d^{2/3}}\int_0^\infty \frac{s'(x-\xi)}{\xi^{1/3}}\,d\xi\right),$$

where $\mu = 3^{2/3}R^{1/3}/\Gamma^2(2/3)$, d is a depth scale for the airflow, $\overline{u} = Q/d$ is a velocity scale with airflow volume flux Q, $\mu_T \approx 0.22 \cdot 10^{-3}\rho Q$ is the eddy viscosity, $R = \rho\overline{u}d/\mu_T$ is a Reynolds number for the flow, and ρ is air density.

In a linear stability analysis, the uniform initial state is always unstable, providing stress exceeds a critical value. The most unstable dimensional wavelength is found to be

$$\ell_D \approx \frac{2\pi d}{0.37R^{1/2}\Theta^{3/2}},$$

where Θ is the Shields stress, equalling τ_0/b, where τ_0 is the stress over a flatbed, and $b \approx \Delta\rho\, g D_s$, and $\Delta\rho$ is the difference between the air and grain densities, and D_s is grain diameter. A common parameterisation is $\tau_0 = \rho K_2 \overline{u}^2$, where $K_2 \approx 10^{-3}$ is dimensionless.

While the above analysis is not be valid once the dune height is high enough to alter the airspeed, and it is well known that separation behind a step or a high enough dune invalidates the assumptions about stress in the separation bubble, the most unstable wavelength may be a useful estimate for slug spacing due to its inverse relationship with slug frequency.

Substituting the values $\overline{u} = 10\,\mathrm{m/s}$, $\rho = 400\,\mathrm{kg\,m^{-3}}$ for coffee bean density, the density of air being one (it may be higher depending on the operating

pressures, which are here assumed close to atmospheric pressure at room temperature), and the height available to airflow $d \approx 0.1\,\mathrm{m}$, gives a flow Reynolds number $\mathrm{Re} \approx 5000$, and a Shields parameter close to critical at $\Theta \approx 0.03$, and a most unstable wavelength $\ell_D \approx 10\,\mathrm{m}$, with a value less than this at pressures above atmospheric. Conveying equipment operates over a range of varying pressures. Two bars of pressure would lead to a most unstable wavelength of just over one metre, for example.

3 Slug Travel and Motion

3.1 Velocity of the Slug

The previous section discusses that the conditions under which slugs form are specific and are likely linked to various interactions within the system. Once slugs have been formed, it is desirable to maintain and preserve them for as long as possible during their travel inside the system. To increase this slug lifespan, we require an understanding of how the various system qualities influence slug travel and motion, so that slugs do not dissipate unnecessarily.

3.2 A Closed-form Solution

Here we consider the flow of granular materials in a pipeline and seek a solution profile that admits travelling wave behaviour. This is to represent slug flow. Analytical results obtained in this section are based on the theory of dense granular flow down an inclined chute. However, we assume a small inclination angle for the chute so that our problem reduces to one-dimensional flow.

To model the flow, we adopt a constitutive model describing the material response, which is based on the theory of classical visco-plasticity. We assume a friction law $\mu(I)$ which is a function of the inertial number I, a dimensionless

parameter (Jop, Forterre, and Pouliquen 2006; Hill, Bhattacharya, and Wu 2021).

In this approach, the granular material is modelled as an incompressible fluid for which the internal (Cauchy) stress tensor

$$\sigma_{ij} = -p\delta_{ij} + \tau_{ij}, \quad \tau_{ij} = \mu(I)p\frac{\dot{\gamma}_{ij}}{|\dot{\gamma}|}, \quad i,j \in \{1,2,3\},$$

where p is the normal pressure, and τ_{ij} represents the deviatoric part. The engineering strain rate tensor $\dot{\gamma}_{ij} = \partial u_i/\partial x_j + \partial u_j/\partial x_i$. The second invariant is $|\dot{\gamma}| = (\dot{\gamma}_{ij}\dot{\gamma}_{ij}/2)^{1/2}$. The inertial number $I = d|\dot{\gamma}|/(p/\rho_s)^{1/2}$, where d is the particle diameter, and ρ_s denotes the particle density. The friction law (Jop, Forterre, and Pouliquen 2006) used is

$$\mu(I) = \mu_0 + \frac{(\mu_\infty - \mu_0)I}{I + I_0},$$

where μ is the coefficient of friction which is a function of I, and μ_0 is the friction for $I = 0$ and μ_∞ is the friction when $I = \infty$.

From the conservation of momentum for any velocity field $\vec{u}$,

$$\rho_s\left(\frac{\partial\vec{u}}{\partial t} + \vec{u}\cdot\nabla\vec{u}\right) = \rho_s\vec{g} + \nabla\cdot\vec{\sigma}. \tag{1}$$

Considering one-dimensional flow, the above-mentioned quantities become

$$\sigma_{xx} = -p + \tau_{xx}, \qquad \tau_{xx} = \mu(I)p\frac{\dot{\gamma}_{xx}}{|\dot{\gamma}|}, \qquad I = \lambda\frac{\partial u}{\partial x},$$
$$\dot{\gamma}_{xx} = \frac{\partial u}{\partial x} + \frac{\partial u}{\partial x} = 2\frac{\partial u}{\partial x}, \qquad |\dot{\gamma}| = \left(\frac{\dot{\gamma}_{xx}\dot{\gamma}_{xx}}{2}\right)^{1/2} = \sqrt{2}\frac{\partial u}{\partial x},$$

where $\lambda = \sqrt{2}d/(p/\rho_s)^{1/2}$. Thus,

$$\tau_{xx} = \left[\mu_0 + \frac{(\mu_\infty - \mu_0)I}{I + I_0}\right]\sqrt{2}p = \left[\mu_0 + \frac{(\mu_\infty - \mu_0)\lambda\frac{\partial u}{\partial x}}{\lambda\frac{\partial u}{\partial x} + I_0}\right]\sqrt{2}p.$$

Here, we look for a solution that admits a travelling wave profile. As a result, we assume that $u(x,t) = F(w)$ where $w = x - kt$ and k is a wave speed. Accordingly,

$$\frac{\partial u}{\partial t} = \frac{dF}{dw}\frac{\partial w}{\partial t} = -k\frac{dF}{dw}, \quad \frac{\partial u}{\partial x} = \frac{dF}{dw}\frac{\partial w}{\partial x} = \frac{dF}{dw}.$$

By ignoring gravity $\vec{g}$ and assuming pressure p is a constant, the momentum equation (1) becomes

$$\rho_s\left(-k\frac{dF}{dw} + F\frac{dF}{dw}\right) = \frac{\partial \sigma_{xx}}{\partial x} = \frac{\partial \tau_{xx}}{\partial x}. \tag{2}$$

Since

$$\tau_{xx} = \left[\mu_0 + \frac{(\mu_\infty - \mu_0)\lambda\frac{dF}{dw}}{\lambda\frac{dF}{dw} + I_0}\right]\sqrt{2}p,$$

so

$$\begin{aligned}
\frac{\partial \tau_{xx}}{\partial x} &= \frac{\partial \tau_{xx}}{\partial w}\frac{\partial w}{\partial x} = \frac{\partial \tau_{xx}}{\partial w} \\
&= \frac{\eta}{(\lambda\frac{dF}{dw} + I_0)}\frac{d^2F}{dw^2} - \frac{\eta\lambda}{(\lambda\frac{dF}{dw} + I_0)^2}\frac{dF}{dw}\frac{d^2F}{dw^2} \\
&= \frac{\eta}{(\lambda\frac{dF}{dw} + I_0)^2}\frac{d^2F}{dw^2}\left(\lambda\frac{dF}{dw} + I_0 - \lambda\frac{dF}{dw}\right) \\
&= \frac{\eta I_0}{(\lambda\frac{dF}{dw} + I_0)^2}\frac{d^2F}{dw^2},
\end{aligned}$$

where $\eta = \sqrt{2}p(\mu_\infty - \mu_0)\lambda$. Thus, differential equation (2) becomes

$$\rho_s\left(-k\frac{dF}{dw} + F\frac{dF}{dw}\right) = \frac{\eta I_0}{(\lambda\frac{dF}{dw} + I_0)^2}\frac{d^2F}{dw^2}. \tag{3}$$

Next, we let $v = \frac{dF}{dw}$ so

$$\frac{d^2F}{dw^2} = \frac{d}{dF}\left(\frac{dF}{dw}\right)\frac{dF}{dw} = v\frac{dv}{dF}.$$

Thus, the differential equation (3) becomes

$$\rho_s(F-k) = \frac{\eta I_0}{(\lambda v + I_0)^2}\frac{dv}{dF},$$

which is rewritten as

$$\alpha(F-k) = \frac{1}{(v+\beta)^2}\frac{dv}{dF}, \quad \text{where} \quad \alpha = \frac{\lambda^2\rho_s}{\eta I_0}, \quad \beta = \frac{I_0}{\lambda}.$$

Using separation of variables,

$$\int \alpha(F-k)dF = \int \frac{1}{(v+\beta)^2}dv$$
$$\iff \quad \alpha\left(\frac{F^2}{2} - kF\right) = -\frac{1}{v+\beta} + K,$$

where K is an arbitrary constant of integration. Since $v = \frac{dF}{dw}$

$$\alpha\left(\frac{F^2}{2} - kF\right) = -\frac{1}{\frac{dF}{dw}+\beta} + K.$$

Rearranging gives

$$\frac{1}{\frac{dF}{dw}+\beta} = K - \alpha\left(\frac{F^2}{2} - kF\right) = K^* - \frac{\alpha}{2}(F-k)^2,$$

where the new constant $K^* = K + \alpha k^2/2$.

Next, we let $G = F - k$ with $dG/dw = dF/dw$, then

$$\frac{1}{\frac{dG}{dw}+\beta} = K^* - \frac{\alpha}{2}G^2 = \frac{\alpha}{2}\left(A^2 - G^2\right),$$

where $A^2 = 2K^*/\alpha$. Thus the above equation becomes

$$\frac{1}{A^2 - G^2} = \frac{\alpha}{2}\left(\frac{dG}{dw} + \beta\right),$$

which simplifies to

$$\begin{aligned}\frac{1}{A^2-G^2}-\frac{\alpha\beta}{2} &= \frac{\alpha}{2}\frac{dG}{dw}\\ \frac{1-\frac{\alpha\beta}{2}A^2+\frac{\alpha\beta}{2}G^2}{A^2-G^2} &= \frac{\alpha}{2}\frac{dG}{dw}\\ \beta\left(\frac{2}{\alpha\beta}-A^2+G^2\right)\frac{1}{A^2-G^2} &= \frac{dG}{dw}.\end{aligned}$$

By separation of variables, we write the above differential equation as

$$dw = \frac{1}{\beta}\frac{(A^2-G^2)}{(B^2+G^2)}\,dG, \quad \text{where} \quad B^2 = \frac{2}{\alpha\beta}-A^2. \tag{4}$$

Since B^2 can be either positive or negative, we consider the solution of the differential equation (4) in the following two cases.

Case 1: $B^2 > 0$ In this case, we solve

$$dw = \frac{1}{\beta}\frac{(A^2-G^2)}{(B^2+G^2)}\,dG.$$

We now use a well-known substitution to allow us to integrate. Let $G = B\tan\theta$ so $dG = B\sec^2\theta\,d\theta$. Thus, $B^2+G^2 = B^2(1+\tan^2\theta) = B^2\sec^2\theta$. Our equation then becomes

$$\begin{aligned}dw &= \frac{1}{B\beta}\left(A^2-B^2\tan^2\theta\right)d\theta\\ &= \frac{1}{B\beta}\left(A^2+B^2-B^2\sec^2\theta\right)d\theta.\end{aligned}$$

Since $B^2 = \frac{2}{\alpha\beta}-A^2$, we have $A^2 = \frac{2}{\alpha\beta}-B^2$. Upon substitution

$$dw = \frac{1}{B\beta}\left(\frac{2}{\alpha\beta}-B^2\sec^2\theta\right)d\theta$$

$$= \frac{2}{\alpha\beta^2 B}\,d\theta - \frac{B}{\beta}\sec^2\theta\,d\theta.$$

Integrating on both sides gives

$$w = \frac{2}{\alpha\beta^2 B}\theta - \frac{B}{\beta}\tan\theta + C,$$

where C is an arbitrary constant. Recalling that $\theta = \arctan\frac{G}{B}$, $G = F(w) - k$ and $w = x - kt$. Thus, the solution to the first case is

$$x - kt = \frac{2}{\alpha\beta^2 B}\arctan\left\{\frac{F(x-kt)-k}{B}\right\} - \frac{(F(x-kt)-k)}{\beta} + C.$$

Case 2: $B^2 < 0$ Letting $B^2 = -D^2$, equation (4) becomes

$$dw = \frac{1}{\beta}\frac{(A^2 - G^2)}{(-D^2 + G^2)}\,dG.$$

Next, we introduce $G = D\tanh\theta$ so $dG = D\,\mathrm{sech}^2\theta\,d\theta$. Thus, $G^2 - D^2 = -D^2(1 - \tanh^2\theta) = -D^2\,\mathrm{sech}^2\theta$. Our equation then becomes

$$\begin{aligned} dw &= -\frac{1}{D\beta}\left(A^2 - D^2\tanh^2\theta\right)d\theta \\ &= -\frac{1}{D\beta}\left(A^2 - D^2 + D^2\,\mathrm{sech}^2\theta\right)d\theta. \end{aligned}$$

Since $-D^2 = \frac{2}{\alpha\beta} - A^2$ we have $A^2 = \frac{2}{\alpha\beta} + D^2$. Upon substitution,

$$\begin{aligned} dw &= -\frac{1}{D\beta}\left(\frac{2}{\alpha\beta} + D^2\,\mathrm{sech}^2\theta\right)d\theta \\ &= -\frac{2}{\alpha\beta^2 D}\,d\theta - \frac{D}{\beta}\,\mathrm{sech}^2\theta\,d\theta. \end{aligned}$$

Integrating on both sides gives

$$w = -\frac{2}{\alpha\beta^2 D}\theta - \frac{D}{\beta}\tanh\theta + C,$$

where C is an arbitrary constant. Recalling that $\theta = \operatorname{arctanh} \frac{G}{D}$, $G = F(w) - k$ and $w = x - kt$, the solution to the second case is

$$x - kt = -\frac{2}{\alpha\beta^2 D} \operatorname{arctanh}\left\{\frac{F(x-kt)-k}{D}\right\} - \frac{(F(x-kt)-k)}{\beta} + C.$$

3.3 Permeating flow rate

While pneumatic conveying is a complex system with multi-phase flow, it is possible to analyse the case of steady-state single slug systems and their individual phases. This section considers multiple approaches to the problem, and existing results based on analysis of the individual phases show that the relationship between mass flow rates of gases into and out of the air pocket behind a slug can be derived using a conservation of mass equation for an ideal gas. This simplified system reveals two crucial features of the single slug system.

1. There is a solution for what input mass flow rate is required to maintain a constant gas pressure/density as a slug propagates down a pipe.
2. The air mass flow rate permeating a slug is, by definition, also the air mass flow rate entering the next downstream slug, and so on.

Knowledge of these two features helps optimise the gas flow rate at the input of the system and examine the stability of multiple slugs.

Considering only the solid phase, the relationship between slug and particle velocities has been derived (Orozovic et al. 2021):

$$v_s = E\,(v_p + c)\,, \tag{5}$$

where v_s is the slug velocity, v_p is the particle velocity, E is the slug to bulk density ratio, which reflects the partially aerated structure of slugs, and c is a propagation velocity of the particle exchange between a slug and a stationary layer.

Equation (5) just reflects that the slug wave (v_s) travels faster than the particles within the wave (v_p), and this is due to the particle exchanges between a slug and its stationary layers, which occur at the propagation velocity c. Using conservation of mass over a slug for the solids phase, a steady slug obeys the relationship (Orozovic et al. 2019)

$$v_s \alpha = Ec, \tag{6}$$

where α is the layer fraction defined as the stationary layer cross-sectional area divided by the pipe cross-sectional area.

Combining equations (5) and (6), the following relation is obtained for steady length slugs between particle velocity v_p, slug velocity v_s and layer fraction α:

$$Ev_p = v_s(1 - \alpha). \tag{7}$$

Equation (7), which is obtained by considering only the solid phase, is utilised to relate to an expression obtained by considering only the gas phase. For the gas phase, we may examine a horizontal pipe and an air pocket behind a slug. Using the ideal gas law, for such a system the following equation must be satisfied:

$$V\frac{dP}{dt} + P\frac{dV}{dt} = RT\frac{dm}{dt} \tag{8}$$

where P is the gas pressure, V is the volume of gas, R is the gas constant, T is gas temperature, and t is time.

Considering the case of steady pressure in the air pocket, the first term on the left-hand side may be neglected, and the rate of change of the volume is just the product $v_s(1 - \alpha)A$, which from equation (7) also equals Ev_pA.

$$\frac{dV}{dt} = v_s(1 - \alpha)A = Ev_pA. \tag{9}$$

So, for steady pressure, substituting (9) into (8), obtains an expression for the rate of change of mass in the air pocket, which is also equal to the difference

in the air mass flow rates entering and leaving the air pocket:

$$\frac{dm}{dt} = \frac{P}{RT} v_p A = \dot{m}_{in} - \dot{m}_{out}, \tag{10}$$

where m is the mass of air in the air pocket, $\dot{m}_{in}$ is the mass flow rate of gas entering the air pocket and $\dot{m}_{out}$ is the permeating flow rate which is leaving the air pocket and entering the slug.

Equation (10) shows at what rate the mass in the air pocket must increase to maintain a constant gas pressure/density during slug motion, and this has found applications (Tan et al. 2008; Orozovic et al. 2020, e.g.). The higher the particle velocity and pressure, the less air permeates a slug. This is especially relevant when examining multiple slug systems, where the permeation flow rate out of one slug is the input flow rate into the next. Furthermore, (10) captures the inverse relationship between particle velocity and pressure noted in the experiments of Lavrinec et al. (2019).

Different applications of equation (10) are of interest in several areas of slug flow, ranging from an expression relating gas pressure and particle velocity, as well as the degree of aeration stemming from the permeating flow rate $\dot{m}_{out}$. Recent work (Lavrinec et al. 2021) that considered numerical simulations and theoretical analysis of single slugs with a steady layer fraction ahead showed that in such cases, there exists a steady slug length. The most interesting potential application of (10) is in expanding (Lavrinec et al. 2021) to the open problem of whether multiple slugs can be individually stable, due to (10) relating the permeating and incoming air mass flow rates for each slug. An application of (10) has recently been considered by Orozovic et al. (2022) who showed that to satisfy gas conservation of mass, multiple slugs of the same steady velocity are not possible, and multiple slugs of different steady velocities are highly unlikely.

During the MISG, the Ergun equation, an extension of Darcy's law for the conservation of momentum in porous media, was considered as a possible additional relation between pressure difference and fluid velocity. However, we

found that the porosity values required for application were well beyond what occurs in slug flow, which was also the conclusion of Lecreps et al. (2014b).

4 Conclusions and Future Work

4.1 Future Work

Due to the complexity of this problem, the MISG provided a preliminary discussion of many important facets of pneumatic conveying systems and an opportunity to develop a relevant and valuable problem overview. However, many of the avenues uncovered will require more time to complete an appropriate analysis. This in-depth analysis can determine the value of the theory for use in pneumatic conveying system design.

We now collect some questions and directions for future research that were uncovered during the Study Group and which are related to work described in the previous sections.

Key Questions

1. When do some of the fluid-based model assumptions required for Navier–Stokes, linear wave theory, etc., break down? What scale systems are our results appropriate for?
2. What is the impact of a varying bed depth on the slug? What happens if the feed rate at the leading edge of the slug is suddenly increased?
3. How fast are the forward-wake particles, and how do they compare in speed to the slug? Does this place limitations on efficiency improvement related to the material size?
4. In the body of the slug, the particles seem to be moving *en masse*, with very little relative motion to one another. Horizontally, the slug as a

whole is pushed forward by the air flowing through the slug, and by the pressure difference across the slug. Opposing these, there is a drag at the pipe walls and on the layer of particles remaining on the pipe base. Vertically there is a downwards force due to gravity balanced by the reaction at the lower pipe surface. Individual particles within the slug are acted upon by interaction with one another, the pressure due to the air flow, and the force of gravity. To what extent is the variable pressure inside the slug responsible for its fluid-like behaviour?

5. In the front of the slug a wedge of particles advances. The bottom of the wedge is formed by the interaction with the bed of stationary particles in front of the slug. In a thin layer between these two regions, particles change speed from being at rest to moving with the slug velocity as they get entrained at the upper surface of the wedge borders with the air above the stationary bed. The slope downwards may be purely due to the necessity of a slope to maintain the 'heap' of the slug. An extra feature here is particles at the front of the wedge accelerating to faster speeds than the speed of particles within the main slug body. This acceleration must be caused by the air pressing through the slug: there are no particles in front to resist this pressure. It is not clear what happens to these accelerated particles. Are they thrown off the front of the slug onto the stationary bed in front to be later re-entrained? Videos suggest so. Or do they get reabsorbed by the slug's forward motion before reaching the bed in front? The slug moves faster than the bodies in its main body. How fast are these forward-wake particles, and how do they compare in speed to the slug itself?

6. At the slug's tail, particles appear to fall out of the slug due to gravity and the lack of particles behind to keep them in place. The back of the slug seems to be collapsing. There appears, in general, to be a gradual slope from the top of the slug down onto the stationary bed of particles behind. Simulations suggest that the particles do not slow down uniformly. Instead, the particles at the bottom of the slug are slowed down faster. This would be expected as they are nearer the

pipe base and are slowed by frictional drag. The particles at the top initially have no such drag. The slowing of particles at the bottom of the tail removes them from below the upper particles, and so these latter particles fall under gravity into the space created. Eventually, these initially high particles are low enough to be affected by friction on the bottom of the pipe, and they all come to rest. Does the slug have greater friction where it contacts the bed than on the sides of the pipe?

7. Is there a circumstance where multiple slugs are theoretically stable within the system? The work in Section 3.3 is an attempt at considering how the formation of new slugs influences the gas flow. Section 3.3 notes this approach was recently applied by Orozovic et al. (2022) to demonstrate that the stability of individual slugs in a system of multiple slugs was doubtful.

Concerning the results within this study and of general importance, the first question helps understand the limitations of the theory and models developed in Sections 2 and 3, that is, a material size/density or velocity/pressure threshold where the fluid-based models no longer provide insight. Questions two, three and four are vital for optimising the mass transport system's efficiency and understanding a slug's behaviour in motion Section 3. Answers to questions five and six would be required to reduce pipeline wear and determine optimal slug speeds (and corresponding pressures/system design), which are consequences of all modelling within this work. The recent resolution of question seven using approaches discussed during the MISG highlights the impact of the study group beyond just the designated week.

4.2 Conclusions

The problem of pneumatic conveying provided an interdisciplinary challenge where various approaches from different branches of mathematics could be utilised. Due to the complexity of the formation of slugs and their motion, many different key areas for investigation were identified in this preliminary

investigation. Through a careful collaborative effort, directions for future work have been established, and members of the MISG2021 are optimistic that this future work will provide a more comprehensive understanding of the interrelation of the components of pneumatic conveying systems. The members of MISG2021 are hopeful that this understanding can be utilised to optimise the design and more efficiently build high-performance pneumatic conveying systems.

Acknowledgements The MISG meeting was supported by ANZIAM. We also thank the University of Newcastle and the Centre for Bulk Solids and Particulate Technologies.

Author addresses

1. **Edward J. Bissaker**, School of Mathematical and Physical Sciences, The University of Newcastle, New South Wales 2308, AUSTRALIA.
mailto:edward.bissaker@uon.edu.au
orcid:0000-0002-1608-286X
2. **Ognjen Orozovic**, School of Engineering, The University of Newcastle, New South Wales 2308, AUSTRALIA.
mailto:ognjen.orozovic@newcastle.edu.au
orcid:0000-0001-5155-9822
3. **Michael H. Meylan**, School of Mathematical and Physical Sciences, The University of Newcastle, New South Wales 2308, AUSTRALIA.
mailto:mike.meylan@newcastle.edu.au
orcid:0000-0002-3164-1367
4. **Fillipe Georgiou**, School of Mathematical and Physical Sciences, The University of Newcastle, New South Wales 2308, AUSTRALIA.
mailto:fillipe.georgiou@uon.edu.au
orcid:0000-0003-4588-5319

5. **Tomas J. Marsh**, School of Mathematical and Physical Sciences, The University of Newcastle, New South Wales 2308, Australia.
mailto:tomas.marsh@uon.edu.au
orcid:0000-0001-8162-5595

6. **James M. Hill**, School of Information Technology and Mathematical, University of South Australia, South Australia 5095, Australia.
mailto:jim.hill@unisa.edu.au
orcid:0000-0003-4623-2811

7. **Mark J. McGuinness**, School of Mathematics and Statistics, Victoria University of Wellington, Wellington 2820, New Zealand.
mailto:mark.mcguinness@vuw.ac.nz
orcid:0000-0003-1860-6177

8. **Winston L. Sweatman**, Massey University, Private Bag 102 904 North Shore Mail Centre, Auckland 0745 New Zealand.
mailto:w.sweatman@massey.ac.nz
orcid:0000-0002-6540-5020

9. **Ngamta Thamwattana**, School of Mathematical and Physical Sciences, The University of Newcastle, New South Wales 2308, Australia.
mailto:natalie.thamwattana@newcastle.edu.au
orcid:0000-0001-9885-3287

References

Bagnold, R.A. (1941). *The physics of blown sand and desert dunes*. Methuen, London (cit. on p. M16).

Benjamin, T.B. (1959). "Shearing flow over a wavy boundary". In: *Journal of Fluid Mechanics* 6.161–205 (cit. on p. M16).

Charru, F. and E.J. Hinch (2006). "Ripple formation on a particle bed sheared by a visous liquid. Part 1. Steady flow." In: *Journal of Fluid Mechanics* 550.1, pp. 111–121 (cit. on p. M16).

Colombini, M. (2004). "Revisiting the linear theory of sand dune formation". In: *Journal of Fluid Mechanics* 502, pp. 1–16 (cit. on p. M16).

Deng, Tong and Michael SA Bradley (2016). "Determination of a particle size distribution criterion for predicting dense phase pneumatic conveying behaviour of granular and powder materials". In: *Powder Technology* 304, pp. 32–40 (cit. on pp. M8, M9).

Engelund, F. (1970). "Instability of erodible beds". In: *Journal of Fluid Mechanics* 42, pp. 225–244 (cit. on p. M16).

Fredsøe, J. (1974). "On the development of dunes in erodable channels". In: *Journal of Fluid Mechanics* 64, pp. 1–16 (cit. on p. M16).

Hill, JM, D Bhattacharya, and W Wu (2021). "SteadyâĂŚstate similarity velocity profiles for dense granular flow down inclined chutes". In: *Granular Matter* 23, p. 27 (cit. on p. M20).

Hilton, JE and PW Cleary (2011). "The influence of particle shape on flow modes in pneumatic conveying". In: *Chemical engineering science* 66.3, pp. 231–240 (cit. on pp. M8, M9, M12).

Jackson, P.S. and J.C.R. Hunt (1975). "Turbulent wind flow over a low hill". In: *Quarterly Journal of the Royal Meteorological Society* 101, pp. 929–955 (cit. on p. M17).

Jop, P, Y Forterre, and O Pouliquen (2006). "A constitutive law for dense granular flows". In: *Nature* 441, pp. 727–730 (cit. on p. M20).

Kennedy, J.F. (1963). "The mechanics of dunes and anti-dunes in erodible-bed channels". In: *Journal of Fluid Mechanics* 16, pp. 521–544 (cit. on p. M16).

Konrad, K (1980). "Prediction of the pressure drop for horizontal dense phase pneumatic conveying of particles". In: *Proc. of Pneumotrasport 5, Paper El* (cit. on p. M10).

Kroy, Kraus, Gerd Sauermann, and Hans J. Herrmann (2002). "Minimal model for sand dunes". In: *Physical Review Letters* 88.5, pp. 054301–1–054301–4 (cit. on pp. M16, M17).

Lavrinec, A et al. (2019). "Observations of dense phase pneumatic conveying using an inertial measurement unit". In: *Powder Technology* 343, pp. 436–444 (cit. on pp. M10, M27).

Lavrinec, A et al. (2021). "An assessment of steady-state conditions in single slug horizontal pneumatic conveying". In: *Particuology* (cit. on p. M27).

Lecreps, I et al. (2014a). "Application of the principles of gas permeability and stochastic particle agitation to predict the pressure loss in slug flow pneumatic conveying systems". In: *Powder Technology* 254, pp. 508–516 (cit. on p. M10).

Lecreps, I et al. (2014b). "Methods for in-situ porosity determination of moving porous columns and application to horizontal slug flow pneumatic conveying". In: *Powder Technology* 253, pp. 710–721 (cit. on p. M28).

Li, K et al. (2014). "Numerical study of horizontal pneumatic conveying: Effect of material properties". In: *Powder Technology* 251, pp. 15–24 (cit. on p. M9).

Meyer-Peter, E. and R. Muller (1948). "Formulas for bedload transport". In: *Proceedings of the Third Annual Conference of the International Association for Hydraulic Research*. The International Association for Hydraulic Research, pp. 39–64 (cit. on p. M17).

Mi, B and PW Wypych (1994). "Pressure drop prediction in low-velocity pneumatic conveying". In: *Powder Technology* 81.2, pp. 125–137 (cit. on p. M10).

Nied, C, JA Lindner, and K Sommer (2017). "On the influence of the wall friction coefficient on void fraction gradients in horizontal pneumatic plug conveying measured by electrical capacitance tomography". In: *Powder Technology* 321, pp. 310–317 (cit. on p. M9).

Orozovic, O et al. (2019). "On the kinematics of horizontal slug flow pneumatic conveying and the relationship between slug length, porosity, velocities and stationary layers". In: *Powder Technology* 351, pp. 84–91 (cit. on p. M26).

Orozovic, O et al. (2020). "Transport boundaries and prediction of the slug velocity and layer fraction in horizontal slug flow pneumatic conveying". In: *Chemical Engineering Science* 227, p. 115916 (cit. on p. M27).

Orozovic, O et al. (2021). "A continuum mechanics derivation of the empirical expression relating slug and particle velocities". In: *Powder Technology* 380, pp. 598–601 (cit. on p. M25).

Orozovic, O et al. (2022). "Individual slugs in a pneumatic conveyor of multiple slugs are likely unstable". In: *Chemical Engineering Science* 250, p. 117365 (cit. on pp. M27, M30).

PCSMS (Feb. 2019). *Pneumatic Conveying Systems Market Size*. Tech. rep., p. 110 (cit. on p. M8).

Pahk, Jae Bum and George E Klinzing (2012). "Frictional force measurement between a single plug and the pipe wall in dense phase pneumatic conveying". In: *Powder Technology* 222, pp. 58–64 (cit. on p. M9).

Pan, R and PW Wypych (1997). "Pressure drop and slug velocity in low-velocity pneumatic conveying of bulk solids". In: *Powder Technology* 94.2, pp. 123–132 (cit. on p. M10).

Pan, Renhu (1999). "Material properties and flow modes in pneumatic conveying". In: *Powder Technology* 104.2, pp. 157–163 (cit. on p. M9).

Parteli, Eric J.R. and Hans J. Herrmann (2007). "Dune formation on the present Mars". In: *Physical Review E* 76:041307 (cit. on p. M16).

Parteli, Eric J.R. et al. (2009). "Dune formation under bimodal winds". In: *PNAS - Proceedings of the National Academy of Sciences of the USA* 106.52, pp. 22085–22089 (cit. on p. M16).

Richards, K.J. (1980). "The formation of ripples and dunes on an erodible bed". In: *Journal of Fluid Mechanics* 99, pp. 597–618 (cit. on p. M16).

Schwämmle, Veit and Hans J. Herrmann (2004). "Modelling transverse dunes". In: *Earth Surface Processes and Landforms* 29.6, pp. 769–784 (cit. on p. M16).

Shaul, Semion and Haim Kalman (2015). "Investigating the conveying mechanism of particulate plugs with stationary layers". In: *Powder Technology* 272, pp. 322–331 (cit. on p. M10).

Shijo, JS and Niranjana Behera (2021). "Review and analysis of solids friction factor correlations in fluidized dense phase conveying". In: *Tribology-Materials, Surfaces & Interfaces* 15.1, pp. 1–9 (cit. on p. M9).

Smith, J.D. (1970). "Stability of a sand bed subjected to a shear flow of low Froude number". In: *Journal of Geophysical Research* 75, pp. 5928–5940 (cit. on p. M16).

Sumer, B. Mutlu and Mehmet Bakioglu (1984). "On the formation of ripples on an erodible bed". In: *Journal of Fluid Mechanics* 144, pp. 177–190 (cit. on p. M16).

Tan, Shengming et al. (2008). "Determination of slug permeability factor for pressure drop prediction of slug flow pneumatic conveying". In: *Particuology* 6.5, pp. 307–315 (cit. on p. M27).

Tsuji, Yutaka, Toshitsugu Tanaka, and T Ishida (1992). "Lagrangian numerical simulation of plug flow of cohesionless particles in a horizontal pipe". In: *Powder Technology* 71.3, pp. 239–250 (cit. on p. M8).

Yi, Jianglin (2001). "Transport boundaries for pneumatic conveying". PhD thesis. Faculty of Engineering, University of Wollongong (cit. on p. M10).

Young, W.R. (2016). *Perturbation Theory*. Scripps Institution of Oceanography, University of California (cit. on p. M15).